

1 Intercomparison of commercial analyzers for atmospheric 2 ethane and methane observations

3 Róisín Commane^{1,2}, Andrew Hallward-Driemeier², Lee T. Murray^{3,4}

4 ¹Department of Earth and Environmental Sciences, Columbia University, New York, NY 10027, USA

5 ²Lamont-Doherty Earth Observatory, Columbia University, Palisades, NY 10964

6 ³Department of Earth and Environmental Sciences, University of Rochester, Rochester, NY 14627, USA

7 ⁴Department of Physics and Astronomy, University of Rochester, Rochester, NY 14627, USA

8 *Correspondence to:* Róisín Commane (r.commane@columbia.edu)

9 Abstract

10 Methane (CH₄) is a strong greenhouse gas that has become the focus of climate mitigation policies in recent years.
11 Ethane/methane ratios can be used to identify and partition the different sources of methane, especially in areas with
12 natural gas mixed with biogenic methane emissions, such as cities. We assessed the precision, accuracy and selectivity
13 of three commercially available laser-based analyzers that have been marketed as measuring instantaneous dry mole
14 fractions of methane and ethane in ambient air. The Aerodyne SuperDUAL instrument performed best of the three
15 instruments but it is large and requires expertise to operate. The Aeris Mira Ultra LDS analyzer also performed well
16 for the price point and small size but required characterization of the water vapor dependence of reported
17 concentrations and careful setup for use. The Picarro G2210-i precisely measured methane but it did not detect the 10
18 ppbv (part-per-billion by volume) increases in ambient ethane detected by the other two instruments when sampling
19 a plume of incompletely combusted natural gas. For long-term tower deployments or those with large mobile
20 laboratories, the Aerodyne SuperDUAL provides the best precision for methane and ethane. The more compact Aeris
21 MIRA can, with careful use, quantify thermogenic methane sources to sufficient precision for mobile and short term
22 deployments in urban or oil and gas areas. We weighed the advantages of each instrument, including size, power
23 requirement, ease of use on mobile platforms, and expertise needed to operate the instrument. We recommend the
24 Aerodyne SuperDUAL or the Aeris MIRA Ultra LDS depending on the situation.
25
26
27
28

Deleted: .

Deleted: cc

Deleted: and space for the large footprint

Deleted: footprint

Deleted: For smaller mobile platforms, t

Deleted: is a more compact analyzer

Deleted: and

Deleted: can

Deleted: , and

Deleted: w

39 **1 Introduction**

40 The atmospheric concentrations of methane (CH₄), a strong greenhouse gas, have been rising at an unprecedented rate
41 in recent years, with record breaking growth rates since 2020 (https://gml.noaa.gov/ccgg/trends_ch4/). Methane has
42 an atmospheric lifetime of ~10 years compared to ~100 years for carbon dioxide (CO₂) and absorbs over 80 times
43 more heat than CO₂ over 20 years (Szopa et al., 2021). Both of these characteristics make the reduction of methane
44 emissions a priority target for short-term reductions in anthropogenic global warming. In recent years, methane has
45 become the target of climate mitigation policies at many levels of government, including international (e.g. founding
46 of the United Nations Environment Programme funded International Methane Emissions Observatory (IMEO) in
47 2022), national (e.g. Inflation Reduction Act, 2022, USA) and local (e.g. New York's Climate Leadership and
48 Community Protection Act, (CLCPA), over 50 cities in the US banning natural gas new construction).

49 Methane sources are categorized as thermogenic (e.g. oil, natural gas, coal mining) or biogenic; which can
50 be both natural (e.g. wetlands) or anthropogenic (e.g. agriculture, landfills, sewage) in origin (Saunio et al., 2020).
51 Each of these methane sources co-emits different trace gas species, which we can use to identify the source of methane.
52 Thermogenic sources of methane, such as natural gas, also contain ethane (C₂H₆) and other hydrocarbons. The
53 incomplete combustion of [liquid \(e.g. natural gas\) or solid \(e.g. coal, wood\) fuels](#), can co-emit high concentrations of
54 carbon monoxide (CO) and other Volatile Organic Compounds VOCs. Biogenic sources of methane do not co-emit
55 ethane, but can emit carbon dioxide (CO₂) and more odorous trace gases such as hydrogen sulfide (H₂S). Therefore,
56 ethane can be used to distinguish between thermogenic (methane/ethane co-emitted) and biogenic (no ethane emitted)
57 sources of methane. Many studies have used methane/ethane ratios to identify natural gas leaks in the natural gas
58 production and distribution networks (Smith et al., 2015; Wunch et al., 2016; Gvakharia et al., 2017; Floerchinger et
59 al., 2019). Methane/ethane observations have also been used for mobile and stationary sampling in urban areas across
60 many countries to identify natural gas leaks separately from biogenically produced methane (McKain et al., 2015;
61 Lamb et al., 2016; Maazallahi et al., 2020; Defratyka et al., 2021).

62 Methane monitoring networks are being developed for city, state and national scales with the goal of
63 evaluating the efficacy of methane reduction policies (Karion et al., 2020; Sargent et al., 2021; He et al., 2019; Mueller
64 et al., 2021). Many of these networks will need to partition the contribution of methane between thermogenic and
65 biogenic sources. In recent years, commercial analyzers have been developed to measure methane and ethane at
66 ambient concentrations and many of these analyzers are marketed as allowing users to attribute the sources of methane.
67 [As far as we can tell, there has not yet been a systematic assessment and characterization of these newly available
68 laser-based ethane spectrometers. There is also little guidance available to those now charged with instrumenting
69 networks and mobile platforms for methane source apportionment.](#)

70 Here, we evaluated three laser-based spectrometers that are marketed to measure ambient [dry mole fractions](#)
71 [of](#) ethane and methane; (i) a cavity enhanced infra-red (IR) absorption spectrometer (Aerodyne Research Inc
72 SuperDual QCI/ICL), (ii) a mid-IR absorption spectrometer (Aeris Technologies Mira Ultra LDS) and (iii) a cavity
73 ring down spectrometer (Picarro G2210-i CRDS). The precision and accuracy of each instrument was evaluated and
74 compared to the advertised performance. We tested the water vapor response and assessed the long-term operation
75 needs of each instrument. Finally, we evaluated the performance of each instrument while sampling urban air at a
76 rooftop site with large natural gas and biogenic emissions in the urban core of New York City in February 2022. We
77 examine the requirements for long-term operation of each analyzer and make recommendations for operation.

78

Deleted: natural gas

Deleted: ((Alvarez et al., 2018; Brandt et al., 2014; Balcombe et al., 2017; Ravikumar et al., 2019)e.g. review of methods described in (Ravikumar et al., 2019).

Deleted: (e.g.

Formatted: Indent: First line: 0.5"

Deleted: ¶

85 **2 Methods**

86 2.1 Description of Analyzers

87 Each of the analyzers described below reports the dry mole fraction of methane and ethane in air using units of
88 ppbv, parts-per-billion by volume, which is the equivalent of nmol mol⁻¹ for an ideal gas.

Formatted: Line spacing: Multiple 1.36 li

89 2.1.1 Aerodyne Research Inc SuperDual

90 Various configurations of Aerodyne laser spectrometers have been used to measure methane and ethane in stationary
91 (McKain et al., 2015), ground-based mobile (Yacovitch et al., 2014), and airborne (Kostinek et al., 2019; Plant et al.,
92 2019) platforms. These spectrometers use a continuous wave interband cascade laser (ICL) based spectrometer to
93 measure methane, ethane and water vapor. ICLs are often used in a two laser system alongside a continuous wave
94 quantum cascade laser (QCL) to measure dry mole fractions of carbon dioxide (CO₂), carbon monoxide (CO), and
95 nitrous oxide (N₂O). Here, we use a SuperDUAL configuration of a two-laser system with a 2L astigmatic Herriott
96 cell (path length 210m) at 50 Torr pressure. The instrument was manufactured in 2015 and refurbished with new lasers
97 in 2020. We use the provided TDLWintel software to fit the absorption spectra and quantify five target gasses and
98 water vapor. The ICL (Laser 1) sweeps from 2988.520 to 2990.625 cm⁻¹ to detect CH₄, C₂H₆ and H₂O. The edge of
99 the ethane absorption feature (2990.081 cm⁻¹) includes a small methane peak (2989.98 cm⁻¹) that is fixed to the value
100 determined from the main fit at 2989.003 cm⁻¹. The QCL (Laser 2) sweeps from 2227.550 to 2228.000 cm⁻¹ and
101 includes absorption features for ¹³CO₂ (2227.605 cm⁻¹), CO (2227.639 cm⁻¹), N₂O (2227.843 cm⁻¹) and H₂O. We use
102 the default water broadening coefficient (WBC) for all species (WBC = 2) except CO (WBC = 1.45). The analyzer is
103 large, and heavy (56 cm x 77 cm x 64 cm; 75kg) and requires an external pump and chiller (to maintain laser
104 temperature stability) that require a stable power source. The instrument has been used extensively and successfully
105 for long-term ground site observations and mobile lab deployments but it is not suitable for smaller/car based mobile
106 sampling. As part of our regular ambient sampling, the Aerodyne SuperDUAL samples nitrogen gas each hour to
107 account for instrument drift, which is especially evident in lower concentration species such as ethane. A smooth
108 spline is fitted to the reported zero for each gas species and subtracted from the 1Hz data.

Deleted: ,

Deleted: value
Deleted: of 2
Deleted: , which is
Deleted: has
Deleted: a
Deleted: ,
Deleted: footprint
Deleted: for

109 2.1.2 Aeris Technologies MIRA Ultra LDS

110 The Aeris Technologies MIRA Ultra LDS (#100209; manufactured July 2021) uses a mid-IR ICL (~3000 cm⁻¹ range)
111 with a multi-pass cell. There are few descriptions of the Aeris MIRA but (Travis et al., 2020) described a similar,
112 portable version of the instrument with an onboard battery (MIRA Pico, not evaluated here). The multi-pass cell (60
113 cm³) has a path length of 13 m and an internal pump maintains the cell pressure at 180 Torr with a ~380 scem flow
114 rate. The small footprint of the rackmount configured analyzer (43 cm x 28 cm x 13 cm; 5 kg) makes it ideal for car-
115 based mobile sampling. The current configuration using a small internal pump is not suitable for sampling below
116 ambient pressure and care should be taken when configuring the system when sampling through long lines on towers.

Deleted: the

117 2.1.3 Picarro G2210-i

118 The Picarro G2210-i (#3441-RFIDS2010, manufactured Aug 2019) is a Cavity Ring Down Spectrometer that
119 measures CH₄, CO₂, C₂H₆, and δ¹³C-CH₄. The instrument uses an external pump to reach a cell pressure of 148 Torr
120 and flow rate of 24 scem through a cavity of 35 cm³ with a path length of up to 30 km

131 (https://www.picarro.com/support/library/documents/g2210i_analyzer_datasheet). [The measurement and reporting](#)
132 [cycle of the Picarro G2210-i are 1Hz. But the low flow rate reduces the instrument response time considerably. We](#)
133 [have corrected for the delay and report methane at 1Hz and we have averaged the ethane to 10s and 5 minutes.](#) Methane
134 data from the instrument has been used on mobile (O'Connell et al., 2019) and stationary (Lebel et al., 2020) platforms
135 and is also mentioned in (Defratyka et al., 2021) but none of these studies have discussed or shown the observed
136 ethane concentrations. The datasheet indicates that the instrument is designed to sample ambient air but may have
137 interferences from elevated concentrations of gas species such as hydrogen sulfide (H₂S) or volatile organic
138 compounds (VOCs).
139

140 2.2 Instrument Evaluation Set-up

141 2.2.1 Humidity

142 The humidity of the sample line for the instruments was varied using a Perma Pure Nafion (™) dryer. Nafion dryers
143 have a semi-permeable membrane separating an internal sample gas stream from a counterflow purge gas stream
144 contained within a stainless-steel outer shell. If the partial pressure of water vapor is higher in the purge gas stream,
145 then water is added to the sample gas stream. A counter flow of air was drawn through the Nafion at ~2000 scem
146 using a vacuum pump. ~~The inlet to the counter flow was alternatively sampling the top of a container of water or dry~~
147 ~~air-conditioned air in the observatory.~~ To achieve the [lowest](#) humidity, dry nitrogen was pushed through the Nafion.
148 The flow rate through the Nafion was controlled using a ball valve and allowed for different rates of changes in the
149 humidity. No liquid water was introduced to the sample lines for the instruments. A range of water vapor from 3% to
150 0.05% was used for all instruments except for the Aeris Mira Ultra LDS ethane data, which was cut off at 1.05% water
151 vapor (for reasons discussed below).
152

153 2.2.2 Calibrations [Against NOAA Standards](#)

154 Each of the instruments [sampled two ambient range cylinders calibrated by the Central Calibration Laboratory \(CCL\)](#)
155 [at the National Oceanographic and Atmospheric Administration \(NOAA\) Global Monitoring Laboratory \(GML\) in](#)
156 [Boulder, CO. CCL maintains the World Meteorological Organization \(WMO\) methane scale \(WMO X2004A\) and an](#)
157 [internal CCL standard for ethane \(C₂H₆-2012\).](#) A dry, compressed air cylinder was used to test multi-hour instrument
158 stability.
159

160 2.2.3 Instrument [Precision](#)

161 We evaluated the instrument [precision](#) by [running a calibrated compressed air cylinder for a 4 hour period and](#)
162 [calculating Allan-Werle variance and precision \(also called continuous measurement repeatability \(CMR\)\)](#) (Defratyka
163 et al., 2021; Yver Kwok et al., 2015). During this time the regular zero for the Aerodyne SuperDUAL was not
164 performed [to allow for direct comparison of all instruments](#). The Aeris MIRA and Picarro G2210-i were humidified
165 (1.7 - 1.9 % H₂O) to allow the Aeris MIRA to report ethane (see Section 3.1). The Aerodyne SuperDUAL was not
166 humidified and reported less than 0.054 % H₂O for the same tests.

Deleted: and t

Deleted: that was at a temperature slightly warmer than the observatory ...

Deleted: driest

Deleted: against

Deleted: standards

Deleted: was calibrated against

Deleted: Stability

Deleted: stability

Deleted: in

177 2.2.4 Nitrogen Tests
178 During regular ambient operation, the Aerodyne SuperDUAL samples nitrogen gas each hour to account for
179 instrument drift. We use the boil off from a large liquid nitrogen dewar, which can be refilled on site, and which
180 contains a variable mole fraction of carbon monoxide (~250 ppbv), and may contain trace levels of oxygen and argon.
181 Regular nitrogen sampling is not required for the long-term operation of either the Picarro G2210-i or the Aeris MIRA.
182 We evaluated the short-term repeatability of the Aeris MIRA and Picarro G2210-i when sampling dry and humidified
183 nitrogen.

184 2.3 Site Description and Sampling of Ambient Urban Air

185 The City University of New York (CUNY) Next Generation Environmental Sensor (NGENS) Observatory is on the
186 rooftop of the 56m building in Hamilton Heights in Harlem. The sampling point is ~93m above sea level on a tower
187 at the south end of the building. The Aerodyne SuperDUAL has been operated at the site over a number of years and
188 was running from early January - June 2022. The site samples urban air that has been influenced by natural gas
189 emissions (both pre and post combustion), wastewater treatment plants (North River to the north-west, Ward Island
190 to the east) and sewer street emissions. During the long-term operation of the Aerodyne SuperDual, nitrogen (liquid
191 nitrogen boil off, N₂) is added as a test of the zero drift in the instrument. For the experiments described here, N₂ was
192 used hourly during ambient sampling and prior to and after the compressed air tank test runs. When the Aerodyne
193 SuperDUAL is operated independently, air is drawn through ~10 m of ½" Synflex tubing at 20 L min⁻¹ using a
194 diaphragm pump before being sub-sampled by the Aerodyne SuperDUAL (flow rate 1.7 L min⁻¹). The use of a separate
195 pump to increase the total flow rate and reduce instrument response times is commonly used for ground operation
196 with longer tubing (e.g. towers). However, the pump also reduces the pressure within the tubing to below ambient
197 pressure, which was a problem when sampling with the smaller pump capacity of the Aeris MIRA. For the work
198 described here, the external pump was removed and the response time through the tubing was reduced to 30s. Each
199 instrument sampled from a Swagelok cross fitting using a ~1m ¼" Synflex tubing.

200 We sampled air from the roof in February, 2022 when ambient air temperatures ranged from below freezing
201 (-9.3°C) to a warm spring day (19°C). The lowest temperatures were also associated with low humidity, which caused
202 problems that were also detected during the humidity testing, so the sample line of the Picarro G2210-i and Aeris
203 MIRA were humidified to >1% water vapor as a work around for these problems.

204 3 Results and Discussion

205 We characterized the laboratory performance of each analyzer with respect to humidity corrections, precision
206 assessment, calibration to NOAA standards and long-term stability, before sampling ambient air in New York City.
207 We used these tests to recommend the best instrument for use in different circumstances.

208 3.1 Characterization of Water Sensitivity

209 All three instruments showed a dependency on water vapor for methane that was statistically significant. Figure 1
210 shows the dependence of the retrieved methane and ethane with the water vapor reported by each instrument for a
211 compressed air cylinder with variable humidity. A linear correction was calculated for methane and ethane for both
212 the Aerodyne SuperDUAL and the Picarro G2210-i but a quadratic dependence was observed for the Aeris MIRA
213 methane (Fig S1). The values of each water vapor correction are shown in Table 1. The Picarro G2210-i needed the

Deleted: Zero-air

Deleted: tests

Deleted: for lower concentration species such as ethane

Deleted: /nmol mol⁻¹

Deleted: .

Deleted: zero

Deleted: but w

Deleted: each instrument's

Deleted: performance

Deleted: the hourly zero air addition for

Deleted: air

Deleted: for air

Deleted: to >0.5% water vapor for the Aeris MIRA and Picarro G2210-i.

Deleted: ambient

Deleted: urban

Deleted: air

Formatted: Line spacing: Multiple 1.36 li

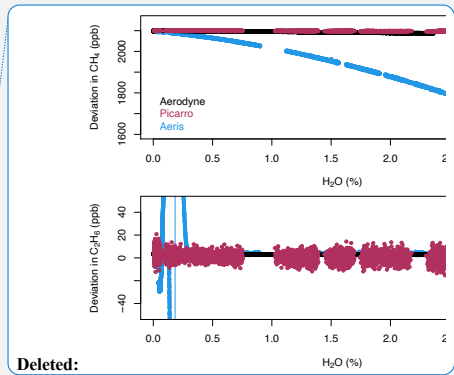
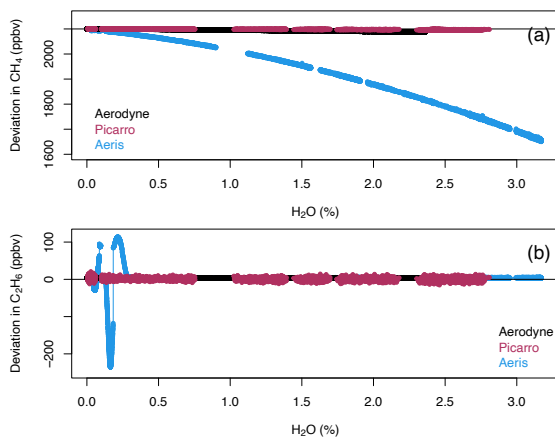
231 smallest absolute correction for methane, and the Aerodyne SuperDUAL reported the smallest correction for ethane.
 232 The SuperDUAL was operated with the default water vapor broadening coefficient for methane and ethane of 2.0.
 233 This correction is likely too large for methane and moving closer to the value of 1.05 recommended by Kostinek et
 234 al., 2019 would reduce the water vapor correction. Here we have applied a linear correction with water vapor to the
 235 observed data that results in a 10 ppbv change in methane but a ~0.08 ppbv change in ethane for 0-2% water vapor.
 236

Deleted: (parts-per-billion by volume; equivalent of nmol mol⁻¹)

237 **Table 1: Summary of water vapor corrections derived for each instrument.**

Instrument	CH ₄ Correction ppbv/% H ₂ O $y = m * [H_2O]$	C ₂ H ₆ ppbv/% H ₂ O $y = m * [H_2O]$	Notes: Using default water broadening coefficients for all instruments before calibration
Aerodyne SuperDUAL	-5.335 ppbv /% H ₂ O	0.042 ppbv /% H ₂ O	
Aeris MIRA Ultra LDS	-25.53 (ppbv/% H ₂ O) ² - 59.22 ppbv/% H ₂ O	0.23 ppbv /% H ₂ O	C ₂ H ₆ only calculated for H ₂ O > 1.05 %
Picarro G2210-i	-1.15 ppbv /% H ₂ O	-0.82 ppbv /% H ₂ O	

Deleted:



Deleted:

238
 239 **Figure 1. Uncorrected (a) methane (ppbv) and (b) ethane (ppbv) vs water vapor (%) for the Aerodyne SuperDUAL**
 240 **(black), Picarro G2210-i (red) and Aeris MIRA Ultra LDS (blue).**
 241

242 We identified two separate, but related, situations with the Aeris MIRA that could prove to be a problem if not
 243 accounted for in operation in certain environments and configurations:

Formatted: Indent: First line: 0"

- 244 (i) The wavelength of the laser is tied to the water vapor absorption peak. When running a dry calibration tank,
 245 the instrument loses frequency lock and the laser wavelength can drift to the point that the ethane peak can
 246 no longer be resolved. The reported ethane concentrations vary between 200 ppbv and -100 ppbv during this
 247 dry air sampling, possibly driven by laser wavelength drift. When the water vapor increases again after a
 248 calibration, the ethane fit is not immediately recaptured. Noise in the reported ethane and methane
 249 concentrations increases significantly below 1.05% water vapor and below 0.5% the ethane fit is completely
 250 lost. [After discussion with engineers at Aeris Technologies, we learned that there are two water vapor peaks](#)

in the spectral window. This problem could be mitigated when sampling dry cylinders by locking to the stronger water vapor absorption peak, which is often saturated during normal operation, or to the methane line directly. Note that locking to the methane line would prevent running zero methane or nitrogen samples as discussed in Section 3.4 below. Either change can be implemented upon request when ordering new analyzers.

Deleted: So t

(ii) For most environments, water vapor in the atmosphere absorbs some of the mid-IR laser power and the laser power of the Aeris MIRA is optimized to achieve maximum sensitivity. However, New York City in February is cold and dry, with very low concentrations of ambient water vapor. Without enough water vapor to attenuate the laser power, the detector can be saturated, leading to no ethane detected and a noisy methane retrieval. This problem can be fixed by reducing the laser power slightly (using the procedure recommended by Aeris Technologies, personal communication) or by humidifying the sample line slightly. We opted for the latter fix for this study. At the other extreme, water vapor closer to 3% can also lead to increased noise in the fitted methane and ethane.

Deleted: engineers

After losing the ethane peak during either of these circumstances, the Aeris MIRA analyzer will often fail to find the peak again until manually re-connected to the internet. We have not identified a cause for this behavior but it was more likely during (ii) and was not a problem after we humidified the sample flow. Using the GPS receiver provided by Aeris also seemed to mitigate the problem.

3.2 Instrument Calibration

Deleted: calibration

Each instrument was calibrated against two NOAA calibration standards after accounting for the water vapor correction described in Section 3.1. A linear fit (OLS, ordinary least squares) was calculated for each species and the span (slope) and zero correction (intercept) and 95% confidence intervals were calculated (Table 2). The span and offset were then applied to each species. As described above, the Aeris MIRA could not report ethane concentrations when sampling a dry tank so the sample line of both the Aeris MIRA and Picarro G2210-i were humidified to water vapor mole fractions between 1.7-1.9 % H₂O. For methane, all three instruments reported a span correction less than 3%, and zero corrections between 3 and 14 ppbv. All three instruments report very similar methane mole fractions for a compressed air tank after all calibration steps were applied. For ethane, the Aeris MIRA and Aerodyne SuperDUAL reported a span less than 7% and offset of less than 2 ppbv. However, the slope and intercept for the Picarro G2210-i were not successfully resolved for the reported 1 Hz data and a two-point linear fit was calculated for the average values reported over the sampling period (Slope 0.427; intercept 4.275). The resulting correction successfully resolved the target gas mole fractions but with a large standard deviation in the 1 Hz data (Fig S2).

Deleted: of

Deleted: 5

Table 2. Calibration span (slope) and zero (intercept) calculated for each instrument reporting at 1 Hz when sampling the NOAA calibration standards. The 95% confidence intervals (CI) for the slope and intercept of an Ordinary Least Squares (OLS) fit are also shown. **The ethane Picarro G2210-i calibration was calculated from the mean of each cylinder measurement (two-point calibration).

Species	Slope	Intercept	95% CI Slope +/-	95% CI Intercept +/-	r ²
Aeris; CH ₄ (ppbv)	0.977	-4.2	0	0.4	1
Aeris; C ₂ H ₆ (ppbv)	0.992	-2.42	0.01	0.07	0.9806

Deleted: (nmol mol⁻¹)

Formatted: Superscript

Picarro; CH ₄ (ppbv)	1.002	1.4	0	0.5	1
Picarro; C ₂ H ₆ (ppbv)**	0.42	4.28			
Aerodyne; CH ₄ (ppbv)	0.969	-13.9	0.001	0.2	1
Aerodyne; C ₂ H ₆ (ppbv)	1.069	0.064	0.001	0.004	0.9996

We evaluated the linearity of the instruments outside our range of calibration standards by comparing the instrument response for the Aerodyne SuperDUAL and Aeris MIRA during the high plumes (as discussed in Section 3.5 below). Fig S3 shows the linearity of 1s methane and 10s ethane for Feb 20-21, 2022 with the Aeris MIRA and Aerodyne SuperDUAL. The methane fit (Slope 1.002) is slightly closer to 1 than the ethane fit (Slope: 1.048 +/- 0.002). The slow response of the Picarro G2210-i meant that it could not represent plumes of ethane at sufficient resolution to allow for valid comparison. While this does not directly test linearity, the strong correlations between reported concentrations from the instruments likely indicates that they retain linear behavior well beyond the range of our calibration standards.

3.3 Instrument Precision

The precision of each analyzer was evaluated by sampling a calibrated compressed air cylinder for four hours. We calculated an Allan-Werle variance (Fig 2) and the observed precision for methane and ethane for each instrument (Table 3; Fig S4-S7).

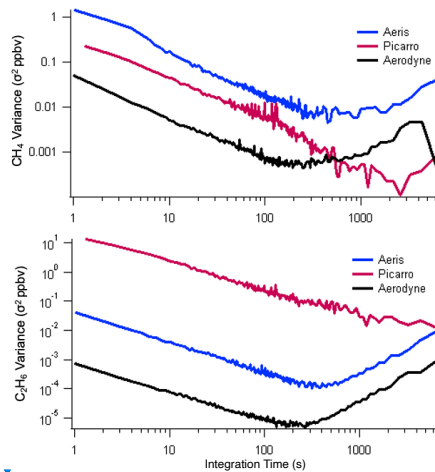
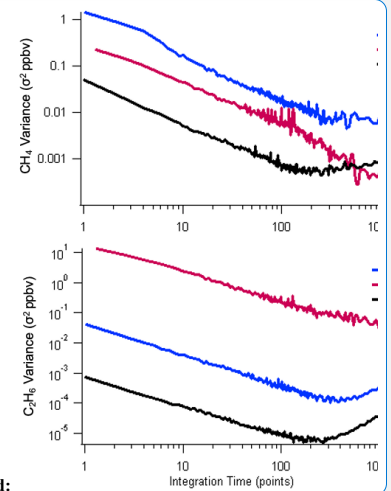


Figure 2. Allan-Werle Variance for (a) methane and (b) ethane for all three instruments when sampling a compressed air cylinder on Feb 17th, 2022 11 am - 3 pm EDT. Each of the tanks was calibrated to NOAA cylinders after water vapor correction. The reported water vapor for the Aerodyne SuperDUAL (black) was below 0.054 %. The Aeris MIRA (blue) and Picarro G2210-i (red) were humidified to water vapor 1.7 – 1.9 %.

Deleted: precision



Deleted:

B17 **Table 3: Summary of various instrument performance metrics. The quoted precisions are from the Product Datasheet for**
 B18 **each analyzer except *Aerodyne SuperDUAL, quoted precision from Kostinek et al., 2019**

Instrument Manufacturer	Flow Rate	CH ₄ Quoted Precision	CH ₄ Observed Precision (100 s)	C ₂ H ₆ Quoted Precision	C ₂ H ₆ Observed Precision (100 s)
Aerodyne SuperDUAL	1500 sccm	0.025 ppbv* (100 s)	0.024 ppbv	0.003 ppbv* (100s)	0.003 ppbv
Aeris MIRA Ultra LDS	380 sccm	0.5 ppbv (1 sec)	0.14 ppbv	1 ppbv (1 sec)	0.02 ppbv
Picarro G2210-i	24 sccm	<0.1 ppbv (5 min)	0.08 ppbv	<1 ppbv (5 min)	0.48 ppbv

B19
 B20 For methane, the Aerodyne SuperDUAL had the best 1 Hz (0.227 ppbv) and 10s (0.072 ppbv) precision with
 B21 a minimum of 0.021 ppbv at 3.2 mins but the variance increased slightly again (but still below 1 ppbv) after about 15
 B22 mins. There were no zeros performed for the SuperDUAL during the precision experiment so this increase in variance
 B23 was not unexpected. The Aerodyne SuperDUAL matched the 100 s precision of (Kostinek et al., 2019) at 0.024 ppbv.
 B24 At 100s, the Aeris LDS precision was 0.14 ppbv and the Picarro G2210-i precision was 0.08 ppbv, both of which
 B25 exceeded their quoted precision of 0.5 ppbv (at 1 s) and 0.1 ppbv (at 5 min).

B26 For ethane, the Aerodyne SuperDUAL had the best 1Hz (0.027 ppbv) and 10s (0.008 ppbv) precision with a
 B27 minimum of 0.002 ppbv at 2.2 mins but the variance increased slightly again (but still below 0.03 ppbv) after about
 B28 15 mins. The Aerodyne SuperDUAL matched the 100s precision of (Kostinek et al., 2019) of 0.003 ppbv. At 100s,
 B29 the Aeris MIRA precision was 0.02 ppbv and the Picarro G2210-i precision was 0.48 ppbv, both of which exceeded
 B30 their quoted precision of 1 ppbv.

B31 **3.4 Long-term Instrument Stability**

B32 We evaluated the stability of frequent additions of nitrogen (liquid nitrogen boil-off free of methane, ethane, CO₂,
 B33 etc.) for all three analyzers. Fig 3 shows the instrument response when sampling dry and humidified nitrogen (methane
 B34 and ethane free). The Aerodyne SuperDUAL was not humidified for the second period (Fig 3c-d) and the noise was
 B35 not significantly different for the two periods (C₂H₆ < 0.01 ppbv; CH₄ < 0.95 ppbv; 1σ s.d.).

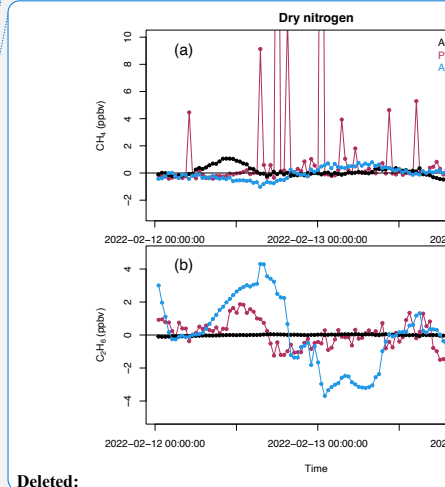
B36 The Aeris MIRA instrument response is statistically different when sampling dry or humidified nitrogen (Fig
 B37 3): The reported ethane goes from varying between -100 and 100 ppbv (with a mean of -3.92 ± 43.8 ppbv; 1σ s.d.)
 B38 when sampling dry nitrogen to -0.05 ± 0.22 ppbv (1σ s.d.) when the nitrogen is humidified to ~1%. This result is
 B39 consistent with the humidity test with compressed air in Figure 1. However, humidifying the nitrogen also affects the
 B40 reported methane, which goes from 0.02 ± 0.5 ppbv (1σ s.d.) when dry to 2.5 ± 17.5 ppbv (1σ s.d.) when humidified.
 B41

- Deleted: Superdual
- Deleted: Q
- Deleted: P
- Formatted Table
- Deleted: nmol mol⁻¹
- Deleted: nmol mol⁻¹
- Deleted: nmol mol⁻¹
- Deleted: nmol mol⁻¹

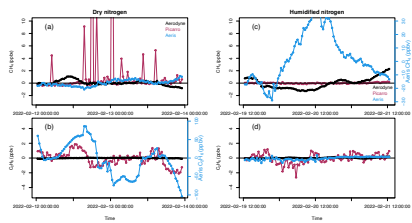
- Deleted: nmol mol⁻¹
- Deleted: The Picarro G2210-i ethane precision is similar to that observed with a Picarro G2201-i analyzer (0.8 ppbv at 1 minute; (Defratyka et al., 2021)).
- Deleted: instrument
- Deleted: stability
- Deleted: zero air
- Deleted: gas
- Formatted: Justified, Indent: First line: 0.5", Line spacing: Multiple 1.36 li, Widow/Orphan control

Deleted: This is also shown as slightly increased noise on the methane at low humidity in Fig S1.

- Deleted: nmol mol⁻¹



Deleted:



366
367
368 **Figure 3: Instrument response when sampling (a-b) dry and (c-d) humidified methane (a, c) and ethane (b, d) in nitrogen.**
369 **Picarro G2210-i (red) and Aeris MIRA (blue). Note the separate right y-axis for the Aeris (b) ethane and (c) methane.**
370 **Also note that the Aerodyne SuperDUAL (black) did not sample humidified nitrogen in c-d.**
371

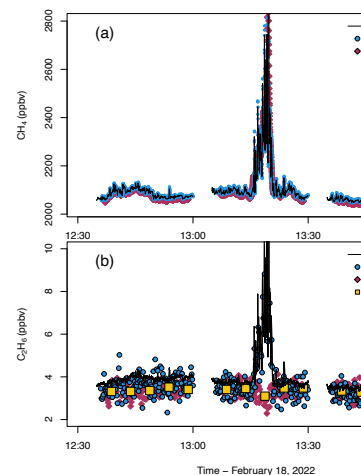
372 The Picarro G2210-i instrument noise is reduced when sampling humidified nitrogen over dry nitrogen (Fig 3),
373 especially for outliers in the reported methane (Fig 3a). The reported ethane goes from -0.082 ± 0.95 ppbv (1σ s.d.)
374 when sampling dry nitrogen to -0.03 ± 1.73 ppbv (1σ s.d.) when the nitrogen is humidified to $\sim 1\%$. The reported
375 methane goes from 1.35 ± 6 ppbv (1σ s.d.) when dry to 0.007 ± 0.08 ppbv (1σ s.d.) when humidified.

376 [Using a Picarro G1301](#), (Nara et al., 2012) [observed a pressure broadening effect when sampling gas with a](#)
377 [range of oxygen and argon that resulted in a \$\sim 2\$ ppb bias in methane. We would expect to see a larger pressure](#)
378 [broadening effect when sampling dry nitrogen free of oxygen and argon, which may explain some of the variability](#)
379 [in Fig 3a. Indeed, there is no increased variability in methane observed by the Picarro G2210-i when sampling from a](#)
380 [compressed air cylinder at low humidity \(Fig 1\(a\)\). For the Aeris MIRA we see different behavior for the methane](#)
381 [and ethane. The ethane results are consistent for both compressed air and nitrogen with more ethane variability at low](#)
382 [humidity. The methane variability is much larger when sampling humidified nitrogen and dry compressed air than](#)
383 [seen when sampling dry nitrogen and humidified compressed air \(see Fig 1 and S1\). In our tests here, the G2210-i](#)
384 [stability for methane is the best of the three analyzers when sampling humidified nitrogen boil off, which indicates](#)
385 [that the addition of nitrogen from a dewar is possible as a long-term zero only if the flow is humidified. However, for](#)
386 [the Aeris MIRA, we observe much more methane variability in humidified nitrogen and lots of ethane variability in](#)
387 [dry nitrogen so we do not recommend using nitrogen as a long-term zero.](#)

388 3.5 Ambient Sampling

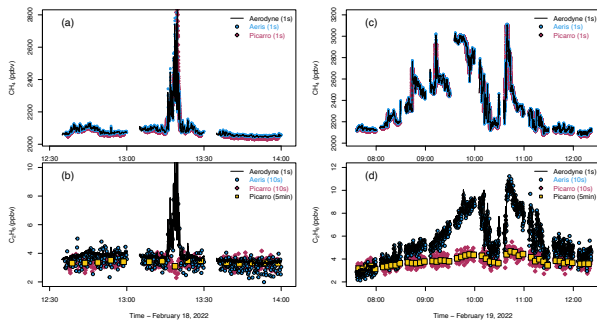
389 [In order to test the suitability of each analyzer to report accurate methane and ethane mole fractions in ambient air, we](#)
390 [ran all instruments sampling ambient air from the CUNY Observatory in Harlem, NY, for 3-4 weeks in February](#)
391 [2022. In general, air is cold and very dry in New York City in winter and \[and it took some time to learn that we had\]\(#\)](#)
392 [to humidify the Aeris MIRA and Picarro G2210-i sample flows in order to record valid data \(see instrument](#)
393 [characterization experiments described above\). The Picarro G2210-i was often reporting negative ethane and negative](#)
394 [correlations of ethane with methane for the first two weeks of observations. We then requested that Picarro engineers](#)
395 [check the instrument and they assured us it was performing as expected. So we have focused on Feb 17-22, 2022 \(see](#)
396 [Fig S8\), when the G2210-i was confirmed to be performing to specification.](#) Figure 4 shows typical examples of the
397 ambient methane and ethane mole fractions observed by all the analyzers when sampling ambient air in February
398 2022.
399
400

Deleted: 3.5 Ambient sampling
Deleted: .
Deleted: we
Deleted: ied
Deleted: in response to the instrument characterization experiments described above
Deleted: The Picarro G2210-i was reporting negative ethane and negative correlations of ethane with methane for the first two weeks of observations so we have focused on the Feb 17-22, 2022 (see Fig S8).



Deleted:

413



414
415 **Figure 4: Ambient sampling for methane (ppbv, top row) and ethane (ppbv, bottom row) for (a-b) a short natural gas**
416 **plume on Feb 18th, 2022 and (c-d) a large scale change in methane and ethane overnight and into the early morning of**
417 **February 19th, 2022. Times in UTC. Aerodyne SuperDUAL (black line), Aeris MIRA (blue circle), Picarro G2210-i (red**
418 **diamond) and Picarro G2210-i averaged to 5 minutes in yellow square. All instruments were corrected for humidity and**
419 **calibrated to NOAA calibration scales.**
420

421 On February 18th a large-scale change in air mass resulted in a drop in ambient air temperature from 15°C to
422 7°C (Fig 4a and b), residential heating increased and a plume of high methane and ethane was intercepted at the
423 observatory for about 10 minutes. The Aerodyne SuperDUAL and Aeris MIRA both responded very similarly;
424 reporting large coincident increases in methane (up to ~2800 ppbv) and ethane (~10 ppbv). The Aerodyne SuperDUAL
425 also reported a large increase in carbon monoxide (CO) up to ~1500 ppbv for the same plume, possibly indicating an
426 incomplete combustion source. The methane reported by the Picarro G2210-i also increased, but with a longer peak
427 duration due to the much slower sampling flow rate (sampling time lags were corrected for previously). However, the
428 ethane surprisingly decreased while sampling the plume.

429 On February 19th ambient air temperatures ranged from -3.7°C at night to -1.2°C in the early morning and
430 wind speeds were low (2-4 m s⁻¹) leading to a build-up of methane and ethane in the atmosphere overnight (Fig 4 c
431 and d). The prolonged elevated methane (to ~3000 ppbv) and ethane (to ~11 ppbv) was easily observed by the
432 Aerodyne SuperDUAL and the Aeris MIRA. The CO also increased (~700 ppbv) to about half of that seen on February
433 18th. The methane reported by the Picarro G2210-i also increased in line with the other reported methane but, again,
434 the Picarro G2210-i was not able to resolve the large increase in ethane, this time indicating an increase in ethane of
435 1-2 ppbv instead of the 7-8 ppbv seen by the other instruments.

436 The trace gases measured by the Aerodyne SuperDUAL indicate that Fig 4 (a and b) shows a post-meter
437 plume of incompletely combusted natural gas, likely emitted close to the observatory. The overnight boundary build-
438 up observed in Fig 4 c and d was coincident with a large increase in other combustion pollutants such as CO. As
439 mentioned in the data sheet for this instrument, it is possible that the co-emitted species of natural gas combustion
440 (such as CO or other volatile organic compounds, VOCs) are acting as an interferent for the Picarro G2210-i ethane
441 retrieval. Our results indicate that the Picarro G2210-i should not be used to selectively measure ethane near
442 combustion sources such as flares, or natural gas power plants or in urban areas that combust natural gas on a large
443 scale. Indeed, care should be taken to ensure that thermogenic sources are not erroneously attributed to biogenic
444 sources with the Picarro G2210-i in urban areas.

Deleted: in the nocturnal boundary layer and

Deleted: during

Deleted: nocturnal boundary layer

Deleted: nocturnal

Deleted: This

Deleted: s

Deleted: i

Deleted: .

453 **4 Conclusions and Recommendations**

454 We evaluated the performance of three commercially available laser-based ethane analyzers: Aerodyne Inc.
455 SuperDUAL, Aeris Technologies MIRA LDS, Picarro Inc. G2210-i. We assessed the precision, accuracy and
456 interferences of each analyzer. We measured ambient air in a cold urban environment with each analyzer and have
457 made recommendations of analyzers based on performance, ease of use and reliability.

458 Across the month, the Aerodyne SuperDUAL reported with the highest precision of all three instruments but
459 requires regular zero air/nitrogen to maintain accuracy. The large size of the instrument and external chiller and large
460 pump mean that it is more suitable for tower/ground-based or large mobile laboratory operation and is not suitable for
461 car-based sampling. There is a smaller size instrument from Aerodyne – the Aerodyne “mini” – which has a
462 methane/ethane precision between that of the SuperDUAL and the Aeris MIRA but this also requires an external
463 chiller and large pump (see <https://www.aerodyne.com/wp-content/uploads/2021/11/Ethane.pdf>; 60s precision of 0.05
464 ppbv CH₄ and 0.015 ppbv C₂H₆). The Aerodyne SuperDUAL also requires expertise to operate and maintain but is
465 the best performing analyzer if the space and expertise are available.

466 The Aeris MIRA was close to the Aerodyne SuperDUAL for precision for methane but was less precise for
467 ethane. The Aeris MIRA pump is small so the analyzer cannot draw against pressures much below ambient pressures,
468 such as those from long sampling lines. Methane required a large water vapor correction. Ethane could only be
469 reported for humidified samples, which affects the calibration protocol most often used in long-term operation. The
470 Aeris MIRA also had some software problems when not connected to the internet, so it requires regular attention.
471 However, overall the Aeris MIRA performed well when sampling plumes of incompletely combusted natural gas and
472 in large-scale ethane build-up overnight in the urban atmosphere. The small size and internal pump also make the
473 analyzer ideal for sampling from small mobile platforms such as cars and bikes (especially the Aeris MIRA LDS Pico,
474 which is the battery-powered version of the analyzer tested here).

475 While the Picarro G2210-i reported precise methane mole fractions and the analyzer performed adequately
476 in many of the tests, it could not detect ambient ethane enhancements of over 5 ppbv observed by the other instruments
477 in the polluted urban atmosphere. When sampling an incompletely combusted natural gas plume, it also reported a
478 reduction in ethane when the other analyzers reported a plume of ~10 ppbv.

479 Overall, we recommend the Aerodyne SuperDUAL or the Aeris MIRA Ultra LDS depending on the situation.
480 For long-term tower deployments or those with large mobile laboratories, the Aerodyne SuperDUAL provides the
481 best precision for methane and ethane. The other reported trace gases in the Aerodyne SuperDUAL, including CO,
482 carbon dioxide (CO₂) and nitrous oxide (N₂O) alongside ethane, also provide a way to more accurately attribute the
483 methane sources. For smaller mobile platforms, the Aeris MIRA is a more compact analyzer, and with careful use,
484 can quantify thermogenic methane sources to sufficient precision for short term deployments in urban or oil and gas
485 areas.

Deleted: or

Deleted: footprint

Deleted: the

Deleted: accuracy

Deleted: increases in a nocturnal urban boundary layer

Deleted: .

492 Data Availability. A permanent link will be added here once the permanent doi is available after the review process.
493 Currently the data from this study is available at: <https://atmoscomp.ldeo.columbia.edu/content/data-sharing>

494 Author Contributions. RC, AHD and LM designed the study, RC and AHD operated the instruments, AHD conducted
495 the tests, RC and AHD analyzed the data. RC prepared the manuscript with input from AHD and LM. The authors
496 declare that they have no conflict of interest.

497 Acknowledgements

498 Funding for this study was provided through contracts to the New York State Energy Research and Development
499 Authority (NYSERDA) grants #160536, #100413, #137484 and #183865, and National Oceanic and Atmospheric
500 Administration (NOAA) grant #NA20OAR4310306. We thank Ricardo Toledo-Crow and the Next Generation
501 Environmental Sciences Observatory of the Advanced Sciences Research Center, City University of New York for
502 Observatory space while conducting the instrument evaluations.
503

504 References

505 Defratyka, S. M., Paris, J.-D., Yver-Kwok, C., Loeb, D., France, J., Helmore, J., Yarrow, N., Gros, V., and
506 Bousquet, P.: Ethane measurement by Picarro CRDS G2201-i in laboratory and field conditions: potential and
507 limitations, *Atmos. Meas. Tech.*, 14, 5049–5069, <https://doi.org/10.5194/amt-14-5049-2021>, 2021.

508 Floerchinger, C., McKain, K., Bonin, T., Peischl, J., Biraud, S. C., Miller, C., Ryerson, T. B., Wofsy, S. C., and
509 Sweeney, C.: Methane emissions from oil and gas production on the North Slope of Alaska, *Atmospheric
510 Environment*, 218, 116985, <https://doi.org/10.1016/j.atmosenv.2019.116985>, 2019.

511 Gvakharia, A., Kort, E. A., Brandt, A., Peischl, J., Ryerson, T. B., Schwarz, J. P., Smith, M. L., and Sweeney, C.:
512 Methane, Black Carbon, and Ethane Emissions from Natural Gas Flares in the Bakken Shale, North Dakota,
513 *Environ. Sci. Technol.*, 51, 5317–5325, <https://doi.org/10.1021/acs.est.6b05183>, 2017.

514 He, L., Zeng, Z., Pongetti, T. J., Wong, C., Liang, J., Gurney, K. R., Newman, S., Yadav, V., Verhulst, K., Miller,
515 C. E., Duren, R., Frankenberg, C., Wennberg, P. O., Shia, R., Yung, Y. L., and Sander, S. P.: Atmospheric Methane
516 Emissions Correlate With Natural Gas Consumption From Residential and Commercial Sectors in Los Angeles,
517 *Geophys. Res. Lett.*, 46, 8563–8571, <https://doi.org/10.1029/2019GL083400>, 2019.

518 Karion, A., Callahan, W., Stock, M., Prinzivalli, S., Verhulst, K. R., Kim, J., Salameh, P. K., Lopez-Coto, I., and
519 Whetstone, J.: Greenhouse gas observations from the Northeast Corridor tower network, *Earth Syst. Sci. Data*, 12,
520 699–717, 2020.

521 Kostinek, J., Roiger, A., Davis, K. J., Sweeney, C., DiGangi, J. P., Choi, Y., Baier, B., Hase, F., Groß, J., Eckl, M.,
522 Klausner, T., and Butz, A.: Adaptation and performance assessment of a quantum and interband cascade laser
523 spectrometer for simultaneous airborne in situ observation of CH₄, C₂H₆, CO₂, CO and N₂O, *Atmos. Meas. Tech.*,
524 12, 1767–1783, <https://doi.org/10.5194/amt-12-1767-2019>, 2019.

525 Lamb, B. K., Cambaliza, M. O. L., Davis, K. J., Edburg, S. L., Ferrara, T. W., Floerchinger, C., Heimbürger, A. M.
526 F., Herndon, S., Lauvaux, T., Lavoie, T., Lyon, D. R., Miles, N., Prasad, K. R., Richardson, S., Roscioli, J. R.,
527 Salmon, O. E., Shepson, P. B., Stirm, B. H., and Whetstone, J.: Direct and Indirect Measurements and Modeling of
528 Methane Emissions in Indianapolis, Indiana, *Environ. Sci. Technol.*, 50, 8910–8917,
529 <https://doi.org/10.1021/acs.est.6b01198>, 2016.

530 Lebel, E. D., Lu, H. S., Speizer, S. A., Finnegan, C. J., and Jackson, R. B.: Quantifying Methane Emissions from
531 Natural Gas Water Heaters, *Environ. Sci. Technol.*, 54, 5737–5745, <https://doi.org/10.1021/acs.est.9b07189>, 2020.

Commented [RC1]: Add NARA

532 Maazallahi, H., Fernandez, J. M., Menoud, M., Zavala-Araiza, D., Weller, Z. D., Schwietzke, S., von Fischer, J. C.,
533 Denier van der Gon, H., and Röckmann, T.: Methane mapping, emission quantification and attribution in two
534 European cities; Utrecht, NL and Hamburg, DE, *Gases/Field Measurements/Troposphere/Physics* (physical
535 properties and processes), <https://doi.org/10.5194/acp-2020-657>, 2020.

536 McKain, K., Down, A., Raciti, S. M., Budney, J., Hutrya, L. R., Floerchinger, C., Herndon, S. C., Nehrkom, T.,
537 Zahniser, M. S., Jackson, R. B., Phillips, N., and Wofsy, S. C.: Methane emissions from natural gas infrastructure
538 and use in the urban region of Boston, Massachusetts, *Proceedings of the National Academy of Sciences*, 112,
539 1941–1946, 2015.

540 Mueller, K. L., Lauvaux, T., Gurney, K. R., Roest, G., Ghosh, S., Gourdji, S. M., Karion, A., DeCola, P., and
541 Whetstone, J.: An emerging GHG estimation approach can help cities achieve their climate and sustainability goals,
542 *Environ. Res. Lett.*, 16, 084003, <https://doi.org/10.1088/1748-9326/ac0f25>, 2021.

543 Nara, H., Tanimoto, H., Tohjima, Y., Mukai, H., Nojiri, Y., Katsumata, K., and Rella, C. W.: Effect of air
544 composition (N₂, O₂, Ar, and H₂O) on CO₂ and CH₄ measurement by wavelength-scanned cavity ring-down
545 spectroscopy: calibration and measurement strategy, *Atmospheric Measurement Techniques*, 5, 2689–2701,
546 <https://doi.org/10.5194/amt-5-2689-2012>, 2012.

547 O’Connell, E., Risk, D., Atherton, E., Bourlon, E., Fougère, C., Baillie, J., Lowry, D., and Johnson, J.: Methane
548 emissions from contrasting production regions within Alberta, Canada: Implications under incoming federal
549 methane regulations, *Elementa: Science of the Anthropocene*, 7, 3, <https://doi.org/10.1525/elementa.341>, 2019.

550 Plant, G., Kort, E. A., Floerchinger, C., Gvakharia, A., Vimont, I., and Sweeney, C.: Large Fugitive Methane
551 Emissions From Urban Centers Along the U.S. East Coast, *Geophysical Research Letters*, 46, 8500–8507,
552 <https://doi.org/10.1029/2019GL082635>, 2019.

553 Sargent, M. R., Floerchinger, C., McKain, K., Budney, J., Gottlieb, E. W., Hutrya, L. R., Rudek, J., and Wofsy, S.
554 C.: Majority of US urban natural gas emissions unaccounted for in inventories, *Proc Natl Acad Sci USA*, 118,
555 e2105804118, <https://doi.org/10.1073/pnas.2105804118>, 2021.

556 Saunio, M., Stavert, A. R., Poulter, B., Bousquet, P., Canadell, J. G., Jackson, R. B., Raymond, P. A.,
557 Dlugokencky, E. J., Houweling, S., Patra, P. K., Ciais, P., Arora, V. K., Bastviken, D., Bergamaschi, P., Blake, D.
558 R., Brailsford, G., Bruhwiler, L., Carlson, K. M., Carrol, M., Castaldi, S., Chandra, N., Crevoisier, C., Crill, P. M.,
559 Covey, K., Curry, C. L., Etiope, G., Frankenberg, C., Gedney, N., Hegglin, M. I., Höglund-Isaksson, L., Hugelius,
560 G., Ishizawa, M., Ito, A., Janssens-Maenhout, G., Jensen, K. M., Joos, F., Kleinen, T., Krummel, P. B., Langenfelds,
561 R. L., Laruelle, G. G., Liu, L., Machida, T., Maksyutov, S., McDonald, K. C., McNorton, J., Miller, P. A., Melton, J.
562 R., Morino, I., Müller, J., Murguía-Flores, F., Naik, V., Niwa, Y., Noce, S., O’Doherty, S., Parker, R. J., Peng, C.,
563 Peng, S., Peters, G. P., Prigent, C., Prinn, R., Ramonet, M., Regnier, P., Riley, W. J., Rosentreter, J. A., Segers, A.,
564 Simpson, I. J., Shi, H., Smith, S. J., Steele, L. P., Thornton, B. F., Tian, H., Tohjima, Y., Tubiello, F. N., Tsuruta, A.,
565 Viovy, N., Voulgarakis, A., Weber, T. S., van Weele, M., van der Werf, G. R., Weiss, R. F., Worthy, D., Wunch, D.,
566 Yin, Y., Yoshida, Y., Zhang, W., Zhang, Z., Zhao, Y., Zheng, B., Zhu, Q., Zhu, Q., and Zhuang, Q.: The Global
567 Methane Budget 2000–2017, *Earth Syst. Sci. Data*, 12, 1561–1623, <https://doi.org/10.5194/essd-12-1561-2020>,
568 2020.

569 Smith, M. L., Kort, E. A., Karion, A., Sweeney, C., Herndon, S. C., and Yacovitch, T. I.: Airborne Ethane
570 Observations in the Barnett Shale: Quantification of Ethane Flux and Attribution of Methane Emissions, *Environ.*
571 *Sci. Technol.*, 49, 8158–8166, <https://doi.org/10.1021/acs.est.5b00219>, 2015.

572 Szopa, S., Naik, V., Adhikary, B., Artaxo, P., Berntsen, T., Collins, W., Fuzzi, S., Gallardo, L., Kiendler-Scharr, A.,
573 Klimont, Z., Liao, P., Unger, N., and Zanis, H.: Chapter 6: Short-lived Climate Forcers, *Climate Change 2021: The*
574 *Physical Science Basis. Contribution of Working Group I to the Sixth Assessment Report of the Intergovernmental*
575 *Panel on Climate Change*, 817–922, <https://doi.org/10.1017/9781009157896.008>, 2021.

- 576 Travis, B., Dubey, M., and Sauer, J.: Neural networks to locate and quantify fugitive natural gas leaks for a MIR
577 detection system, *Atmospheric Environment: X*, 8, 100092, <https://doi.org/10.1016/j.aeaoa.2020.100092>, 2020.
- 578 Wunch, D., Toon, G. C., Hedelius, J. K., Vizenor, N., Roehl, C. M., Saad, K. M., Blavier, J.-F. L., Blake, D. R., and
579 Wennberg, P. O.: Quantifying the loss of processed natural gas within California's South Coast Air Basin using
580 long-term measurements of ethane and methane, *Atmospheric Chemistry and Physics*, 16, 14091–14105, 2016.
- 581 Yacovitch, T. I., Herndon, S. C., Roscioli, J. R., Floerchinger, C., McGovern, R. M., Agnese, M., Pétron, G., Kofler,
582 J., Sweeney, C., Karion, A., Conley, S. A., Kort, E. A., Nähle, L., Fischer, M., Hildebrandt, L., Koeth, J., McManus,
583 J. B., Nelson, D. D., Zahniser, M. S., and Kolb, C. E.: Demonstration of an Ethane Spectrometer for Methane Source
584 Identification, *Environ. Sci. Technol.*, 48, 8028–8034, <https://doi.org/10.1021/es501475q>, 2014.
- 585 Yver Kwok, C., Laurent, O., Guemri, A., Philippon, C., Wastine, B., Rella, C. W., Vuillemin, C., Truong, F.,
586 Delmotte, M., Kazan, V., Darding, M., Lebègue, B., Kaiser, C., Xueref-Rémy, I., and Ramonet, M.: Comprehensive
587 laboratory and field testing of cavity ring-down spectroscopy analyzers measuring H₂O,
588 CO₂, CH₄ and CO, *Atmos. Meas. Tech.*, 8, 3867–3892,
589 <https://doi.org/10.5194/amt-8-3867-2015>, 2015.
- 590